

## Molecularly Imprinted Electrochemical Sensor for Determination of Stanozolol in Human Plasma

Lixin Zheng<sup>1</sup>, Chunjuan Lu<sup>2,\*</sup>

<sup>1</sup> Teacher Education College, Shaoxing University, Shaoxing, Zhejiang, 312000, China

<sup>2</sup> Zhejiang A&F University, Hangzhou, 311300, China

\*E-mail: [cdtylmj@sina.com](mailto:cdtylmj@sina.com)

Received: 11 August 2022 / Accepted: 10 October 2022 / Published: 20 October 2022

The current study's objective was to create an electrochemical sensor based on molecularly imprinted polymers (MIP) and carbon nanotubes (CNTs) modified glassy carbon electrode (MIP/CNTs/GCE) for sensitive and precise detection of stanozolol (SNZ) as a doping agent in human plasma from athletes. For preparation of the MIP/CNTs/GCE as an electrochemical sensor, a MIP thin film on GCE with modified CNTs was prepared using the electropolymerization method. XRD and SEM structural analyses of nanostructures revealed that MIP was electropolymerized on CNTs successfully. Amperometry and differential pulse voltammetry (DPV) studies showed that CNTs and the molecularly imprinted polymer matrix had a positive synergistic electrocatalytic effect to produce a stable and selective determination of SNZ. Additionally, the linear concentration range of 0-120  $\mu\text{M}$  was established, and the sensitivity and detection limit of  $0.30444\mu\text{A}/\text{ng}\cdot\text{mL}^{-1}$  and 0.009 ng/mL, respectively, were estimated. Analytical results showed the recovery (99.30% to 99.60%) and RSD (3.81% to 4.42%) values were acceptable, and this method was appropriate for valid and precise practical analyses in blood plasma and clinical samples. The precision and validity of MIP/CNTs/GCE were successfully examined for the purpose of determining the level of SNZ in blood plasma samples from healthy volunteer bodybuilders who were taking SNZ medication.

**Keywords:** Molecularly Imprinted Polymers; Carbon Nanotubes; Selectivity; Electropolymerization; Stanozolol; Bodybuilding; Amperometry

### 1. INTRODUCTION

The synthetic anabolic steroid Stanozolol (SNZ) is produced artificially by condensation of the 3-keto-aldehyde moiety of oxymetholone with hydrazine [1, 2]. It has androgenic action and is an orally active anabolic steroid [3, 4]. In the liver, SNZ is converted into conjugates of glucuronide and sulfate. SNZ works by lowering the production of a peptide known as bradykinin, which causes inflammation and causes blood vessels to burst and leak [5, 6]. Hereditary angioedema, which

produces episodes of swelling of the face, limbs, genitalia, intestinal wall, and throat, is treated with SNZ [7, 8]. The frequency and intensity of these attacks might be lessened with SNZ. Additionally, it is utilized to treat osteoporosis, anemia, and other health problems [9, 10].

Athletes can get stronger, gain muscle mass, increase acceleration, recover from exercises and other physical stresses more quickly, and become more forceful by using the steroid SNZ, which mimics testosterone and increases muscle mass [11-13]. One of the most often overused anabolic steroids, SNZ has been linked to a number of physical and psychological side effects. Abuse of anabolic steroids like SNZ can make people angry and result in high blood pressure, liver issues, sagging breasts in women, impotence and decreased sperm production in males, kidney failure, and heart disease [14, 15]. It can also make people more prone to aggression. The World Anti-Doping Agency forbids its use in sports (WADA). Synthetic anabolic steroids were formerly only used for doping by professional athletes and bodybuilders [16, 17].

Therefore, it is crucial to determine the SNZ level in clinical and pharmaceutical samples. The determination of SNZ, however, has been studied using LC-MS/MS [18], LC/MS [19], LC-EI-MS/MS [20], SPE-LC-HRMS [21] and ELISA [22]. Due to the presence of several chemical components in biological fluids and pharmaceutical samples, the selectivity of these sensors is limited. The development of imprinted binding sites in molecular imprinted polymer (MIP)-based electrochemical sensors has been shown to result in high selectivity; hence, it would be helpful to understand the chemical makeup of these sites [23-26]. The objective of the current study is to create an electrochemical sensor based on CNTs and MIP-modified GCE for sensitive and precise detection of SNZ as a doping agent in human plasma from athletes.

## 2. EXPERIMENT

### 2.2. Preparation of MIPs/CNTs/GCE

Prior to alteration, a mirror-like surface was achieved by 20 minutes of continuous polishing of a GCE surface (3 mm in diameter) with  $\text{Al}_2\text{O}_3$  slurry powder (0.05  $\mu\text{m}$ , 99.99%, Sigma-Aldrich). The GCE was then ultrasonically washed with deionized water before being exposed to a mixture of ethanol (99 percent, Merck Millipore, Germany) and deionized water for 10 minutes. After being homogeneously mixed with 50 mL of dimethylformamide (DMF, 99.8%, Merck Millipore, Germany) for 15 minutes, 5 mg of CNTs (Jiaxing ACG Composites Co., Ltd., China) were placed onto the surface of the GCE. The modified GCE was then dried under an infrared heat lamp in order to evaporate the solvent. Then, on an electrochemical workstation potentiostat (made by Xiamen Tob New Energy Technology Co., Ltd., China), electropolymerization was carried out in a standard three-electrode electrochemical cell that contained clean CNTs/GCE as the working electrode, Pt wire as the counter, and Ag/AgCl (3 M KCl) as the reference electrode [27]. The electrolyte was made with 0.1 M phosphate buffer solution (PBS) containing 50 mM aniline (99.5%, Sigma-Aldrich) and 10 mM SNZ. Through CV electropolymerization at a potential range of 0.15 to 1.1 V and a scanning rate of 20 mV/s for 5 cycles, the MIP film was created on the surface of CNTs/GCE. Following electropolymerization, the modified electrode was submerged for 5 minutes under magnetic stirring in a 9:1 volume ratio of

methanol (99.9 %, Sigma-Aldrich) and acetic acid (99.0 %, Sigma-Aldrich) to remove the template molecules from the polyaniline film.

## 2.2. Measurement instruments

A differential pulse voltammetry (DPV) and electrochemical workstation potentiostat galvanostat (CS350, Wuhan Corrtest Instruments Corp., Ltd., China) was used to measure amperometry. The electrochemical workstation has a three-electrode electrochemical cell with a working electrode, a counter electrode, and a reference electrode made of Ag/AgCl (bare or modified GCE). All electrochemical tests were conducted in 0.1M phosphate buffer solution (PBS) electrolyte (pH 7.0), which was made from an equal amount of 0.1M NaH<sub>2</sub>PO<sub>4</sub> (99%) and 0.1M Na<sub>2</sub>HPO<sub>4</sub> (99%). A German Bruker D8-FOCUS X-Ray Diffraction system was used to obtain the X-ray diffraction (XRD) patterns. Using a JEOL JSM 6060 microscope, scanning electron microscopy (SEM) images of the sample morphology were provided.

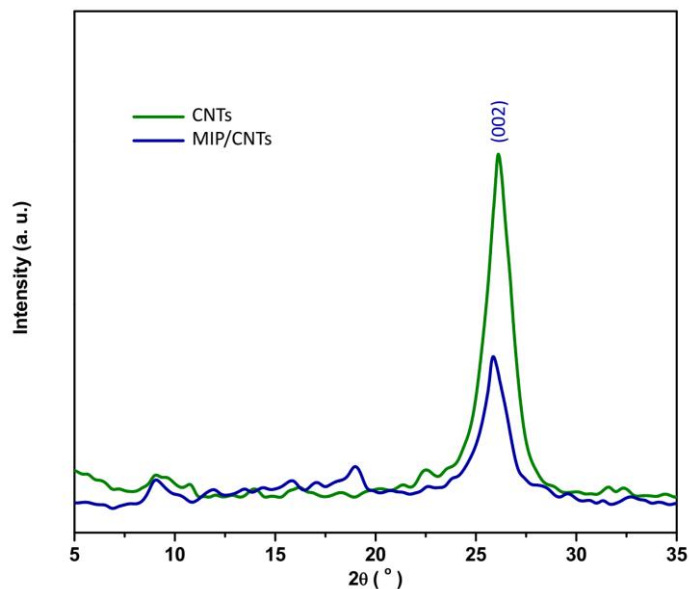
## 2.3. Study the real sample

After injection, Winstrol (TN Pharma, USA) had 75 mg/mL of SNZ, according to the accuracy and validity of MIP/CNTs/GCE for determining SNZ in prepared genuine samples from blood plasma samples that originated from healthy volunteer bodybuilders. The active half-life of a SNZ injection is roughly 24 hours. As a result, blood was drawn six hours following the SNZ injection. The blood sample was centrifuged for 8 minutes at 1200 rpm. The supernatant from phase separation was filtered and used to make 0.1 M PBS (pH 7.0). The solution was subsequently utilized as an electrochemical electrolyte.

# 3. RESULTS AND DISCUSSION

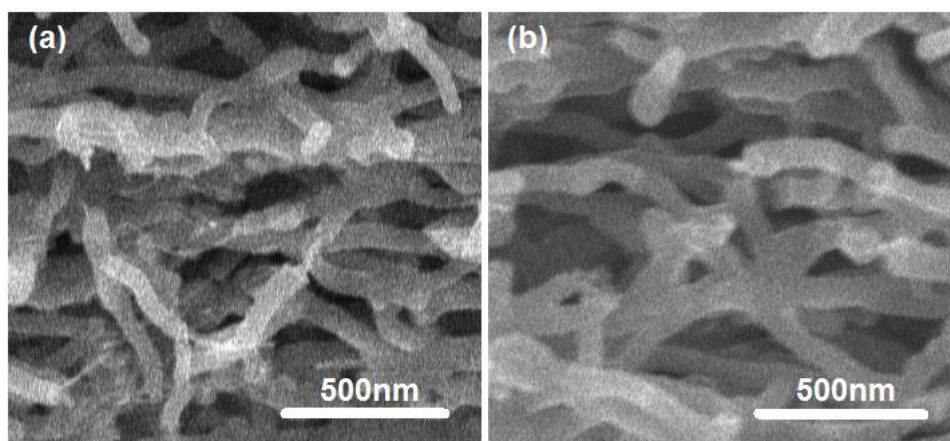
## 3.1. Structural studies of CNTs and MIP/CNTs nanostructures modified GCE

Figure 1 shows the XRD patterns of powder CNTs and MIP/CNTs. As can be seen, the sharp diffraction peak in both XRD patterns corresponds to the graphitic carbon in CNTs with plane (002) (JCPDS card no. 75-1621) and is visible at around 26.10° [28]. However, the MIP/CNTs XRD pattern's diffraction peak strength has somewhat diminished, indicating that amorphous MIP has electropolymerized on the surface of CNTs [29, 30].



**Figure 1.** The XRD patterns of powder CNTs and MIP/CNTs

Figure 2 displays the SEM micrographs of the CNTs/GCE and MIP/CNTs/GCE. Figure 2a's SEM micrograph of the CNTs/GCE shows that the GCE surface has been transformed by densely enwrapped CNTs with distinctive tubular networks and an average diameter of 55 nm. According to Figure 2b, MIP was successfully electropolymerized on CNTs since the average diameter of MIP/CNTs is 85 nm, which is larger than the average diameter of pure CNTs modified by GCE. A wide accessible surface area is also provided by the 1D structure of CNTs, which makes them excellent nanostructures to stop MIP from aggregating or restacking [31, 32].

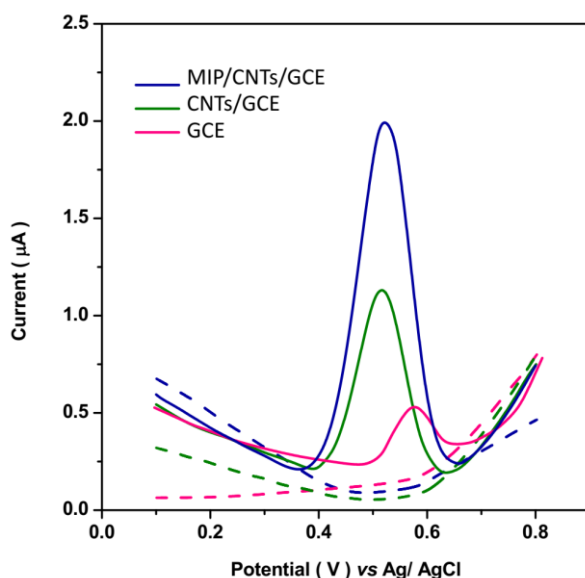


**Figure 2.** The SEM micrographs of (a) CNTs/GCE and (b) MIP/CNTs/GCE.

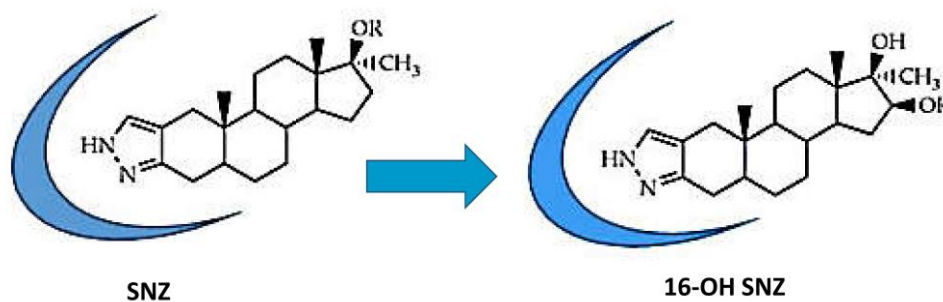
### 3.2. Electrochemical studies

Figure 3 displays the DPV curves of unaltered GCE, CNTs/GCE, and MIP/CNTs/GCE at potentials ranging from 0.10 V to 0.80 V at a scanning rate of 15 mV/s in 0.1 M PBS (pH 7.0), both

with and without SNZ solutions. When there is no SNZ solution in the electrochemical cell, none of the electrodes show any distinct peak in the DPV curves. Anodic peaks are observed on the DPV curves of GCE, CNTs/GCE, and MIP/CNTs/GCE, respectively, at 0.57 V, 0.53 V, and 0.52 V when the SNZ solution is added to the electrolyte of an electrochemical cell. It is hypothesized that these peaks are brought on by the oxidation of stanzolol's hydroxy ketone [33, 34]. Casati et al. also suggested that SNZ compounds, with a spacer arm at position 17 $\beta$ -OH, can expose the pyrazole ring to the sensing system which in the SNZ structures acts as a recognition region site and will allow detection SNZ (Figure 4). It is clear that MIP/CNTs/GCE has a higher electrocatalytic current than bare GCE and CNTs/GCE, and that its peak current occurs at the lowest potential. It demonstrates the advantageous electrocatalytic synergy between CNTs and the molecularly imprinted polymer matrix. To produce voids in the polymers that are sterically and chemically complementary to the templates, monomers are first compounded with the templates (analytes) and then polymerized to make a synthetic polymer matrix. After the templates are removed, the specially designed binding cavities can distinguish the templates from their analogs [35, 36]. CNTs with excellent electrical conductivity, high surface area, and chemical and mechanical stability can compensate for MIPs' lack of conductivity and electrocatalytic activity [37-39]. The density of recognition sites and conductivity of MIP-based sensors can be improved through electropolymerization of MIP on CNTs, which is essential to rebind the analyte molecules and speed up the electron transmission [37, 40]. Moreover, CNTs defect sites provide the functional groups that can react with reactive end groups MIP [41]. Therefore, the modification of CNTs with MIP thin film promotes the electrocatalytic activity of MIP/CNTs/GCE. Thus, MIP, CNTs, and GCE were subjected to the following electrochemical assays.



**Figure 3.** the DPV curves of unmodified GCE, CNTs/GCE and MIP/CNTs/GCE at potentials between 0.10 V and 0.80 V at a scanning rate of 15 mV/s in 0.1 M PBS (pH 7.0) in both of absence (dashed line) and presence (solid line) of SNZ solutions.



**Figure 4.** The suggested oxidation mechanism of stanozolol

In an electrochemical cell containing 0.1 M PBS, Figure 5 shows the amperometric reactions of MIP/CNTs/GCE following repeated injections of 5 ng/mL SNZ solutions at potentials of 0.52 V. (pH 7.0). With each injection of 5 ng/mL SNZ solution, it is demonstrated that the amperometric current increases, demonstrating a quick and stable response from MIP/CNTs/GCE. A sensitivity of  $0.30444\mu\text{A}/\text{ng}\cdot\text{mL}^{-1}$  for MIP/CNTs/GCE toward SNZ is achieved, as evidenced by the calibration plot of Figure 5's inset, which shows that peak current intensities of amperometric responses climb linearly over the concentration range of 0 to 120  $\mu\text{M}$ . The detection limit can also be estimated to be 0.009 ng/mL. In Table 1, these sensing characteristics are contrasted with newly published SNZ sensor results [42, 43]. As can be shown, MIP/CNTs/GCE demonstrates the lowest detection limit value among LC-MS/MS, LC/MS, LC-EI-MS/MS, SPE-LC-HRMS, and ELISA-based sensors in addition to having a relatively broad linear range. As a result, the combined use of MIP as selective electrochemical platforms and CNTs as an electroactive redox probe at the surface of the MIP/CNT modified electrode accounts for the present work's significant innovation in comparison to other published results of SNZ sensors.

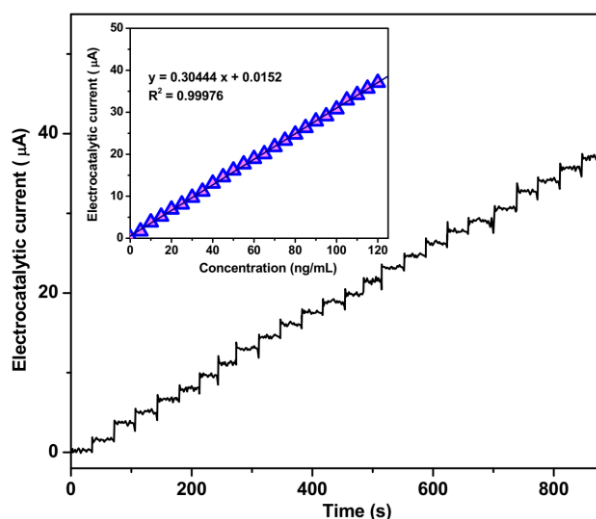


**Figure 5.** The amperometric responses and corresponding calibration plot of MIP/CNTs/GCE to consecutive injections of 5 ng/mL SNZ solutions at potentials of 0.52 V in an electrochemical cell containing 0.1 M PBS (pH 7.0).

**Table 1.** The performance of electrochemical sensor for determination of SNZ in present work and recently released outcomes of SNZ sensors.

Electrode	Technique	LOD (ng/mL)	Linear range (ng/mL)	Ref.
MIP/CNTs/GCE	Amperometry	0.009	0 to 120	present work
C-18 column	LC-MS/MS	0.125	0.125 - 25	[44]
C18 column	LC/MS/MS	1	1-30	[18]
Supelcosil LC-8 DB column	LC/MS	0.3	---	[19]
C-18e column	LC-EI-MS/MS	2	5-250	[20]
Kinetex EVO C-18 column	SPE-LC-HRMS	0.1	1-100	[21]
SNZ-Ab/SPE	ELISA	0.175	0.64 –2	[22]

LC-MS/MS: Liquid chromatography tandem mass spectrometry; LC-MS: Liquid chromatography-mass spectrometry; SNZ-Ab/SPE: anti-stanozolol/Screen Printed Carbon Electrode; LC-EI-MS/MS: Liquid chromatography-electrospray ionization tandem mass spectrometry method; SPE-LC-HRMS: Solid-phase extraction-liquid chromatography with high resolution mass spectrometer; ELISA: enzyme-linked immunosorbent assay

The MIP/CNTs/GCE system's sensitivity as an SNZ electrochemical sensor was assessed in the presence of numerous drugs and compounds that are present in biological fluid. The results of electrocatalytic signal amperometric measurement employing MIP/CNTs/GCE at a potential of 0.52 V in 0.1 M PBS (pH 7.0) in response to consecutive injections of 5 ng/mL SNZ solution and 20 ng/mL interfering species are shown in Table 2. Interferences can happen when there is a lack of specificity in the electrode surface and the kind of electrolyte, as well as when these substances decrease and/or oxidize at potentials close to the SNZ [45, 46]. While adding interfering species to the electrolyte solution does not provide any visible electrocatalytic signal, adding SNZ solution to an electrochemical cell does produce a noticeable electrocatalytic signal. Molecular hosts that provide cavities for selective binding with catalytically active functional groups within the cavity in the proper vicinity to the reactive groups of the bound substrate are used during the electropolymerization of molecularly imprinted polymer on CNTs. It dramatically improves selectivity [47]. Additionally, better accessibility of the particular receptor-recognition contacts for the analyte and less resistance to mass transfer are provided by the synergistic effect of the recognition sites of MIP film on CNTs [35, 48].

**Table 2.** The outcomes of electrocatalytic signal of amperometric measurement using MIP/CNTs/GCE at potential of 0.52 V in 0.1 M PBS (pH 7.0) to sequential injections of 5 ng/mL SNZ solution and 20 ng/mL of interfering species.

Substance	Added (ng/mL)	Amperometric signal ( $\mu$ A) at 0.52 V	RSD
SNZ	5	1.5221	$\pm$ 0.0074
Ascorbic acid	20	0.0529	$\pm$ 0.0021
Dopamine	20	0.0201	$\pm$ 0.0015
Glucose	20	0.0406	$\pm$ 0.0019
Lactose	20	0.0224	$\pm$ 0.0017

Folic acid	20	0.0311	±0.0018
Cholesterol	20	0.0293	±0.0012
Uric acid	20	0.0447	±0.0022
Lactic acid	20	0.0225	±0.0012
Acetaminophen	20	0.0195	±0.0019
Dehydroepiandrosterone	20	0.0325	±0.0019
Codeine	20	0.0374	±0.0018
Norepinephrine	20	0.0286	±0.0016
Albumin	20	0.0198	±0.0012
Fe <sup>2+</sup>	20	0.0263	±0.0011
Ca <sup>2+</sup>	20	0.0320	±0.0015
Zn <sup>2+</sup>	20	0.0167	±0.0010
Mg <sup>2+</sup>	20	0.0353	±0.0012

In order to measure the concentration of SNZ in blood plasma samples from healthy volunteer bodybuilders who were receiving SNZ injections, the accuracy and validity of MIP/CNTs/GCE were investigated. Figure 6 shows the outcomes of an amperometric test carried out at a potential of 0.52 V on blood plasma from bodybuilders prepared in 0.1 M PBS (pH 7.0). The SNZ level in the processed sample is 0.16ng/mL, as shown by the appropriate calibration plot in inset Figure 6. The results of the analysis using the conventional addition approach are shown in Table 3. The results show that the recovery (99.30% to 99.60%) and RSD (3.81 percent to 4.42 percent) values are acceptable and that this approach is suitable for practical studies in blood plasma and clinical samples that are valid and accurate.

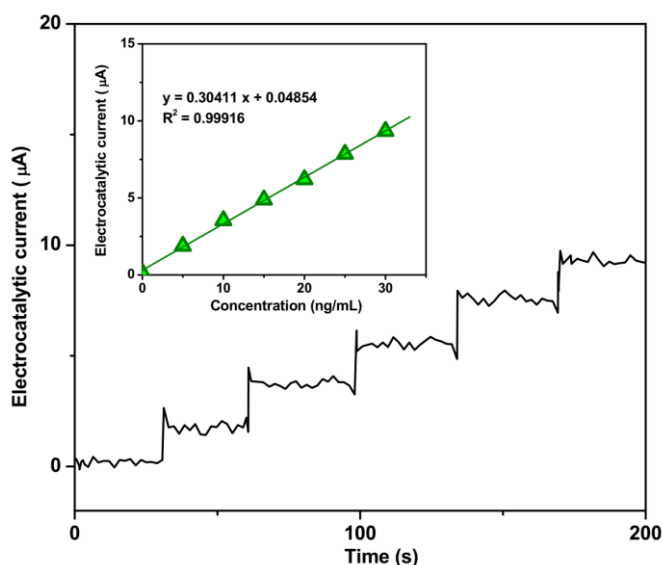


**Figure 6.** The amperometric responses and corresponding calibration plot of MIP/CNTs/GCE to consecutive injections of 5 ng/mL SNZ solutions at potentials of 0.52 V in in 0.1 M PBS (pH 7.0) prepared sample from bodybuilder blood plasma.

**Table 3.** The obtained analytical findings of determination of SNZ in the prepared real samples of bodybuilder blood plasma.

spiked (ng/mL)	detected (ng/mL)	Recovery (%)	RSD (%)
0.00	0.16	---	4.13
5.00	5.13	99.40	4.21
10.00	10.12	99.60	3.81
15.00	15.07	99.40	4.25
20.00	20.02	99.30	4.42

#### 4. CONCLUSION

Finally, the current study described the synthesis of MIP/CNTs/GCE as an electrochemical sensor for the precise and sensitive detection of SNZ in athlete blood plasma. MIP thin films were prepared using the electropolymerization process and applied to GCE with CNT modifications. The 1D structure of CNTs provided the optimal nanostructures to prevent the aggregation or restacking of MIP in order to provide a broad accessible surface area, according to structural studies that showed the electropolymerization of MIP on CNTs to be successful. Electrochemical tests demonstrated the CNTs' and the molecularly imprinted polymer matrix's advantageous synergistic electrocatalytic effect on the selective and stable determination of SNZ. Additionally, the linear concentration range of 0-120  $\mu\text{M}$  was established, and a sensitivity and detection limit of  $0.30444\mu\text{A}/\text{ng}\cdot\text{mL}^{-1}$  and 0.009 ng/mL, respectively, were estimated. Analytical results showed the recovery and RSD values were acceptable, and this method was appropriate for valid and precise practical analyses for detecting SNZ as a doping agent in blood plasma and clinical samples of athletes. The precision and validity of MIP/CNTs/GCE were successfully examined for the purpose of determining the level of SNZ in blood plasma samples from Volcaner bodybuilders who were taking SNZ medication.

#### References

1. C.R. Sharma, N.H. Balasinor and L.S. Inamdar, *Steroids*, 165 (2021) 108752.
2. M. Yang, C. Li, Y. Zhang, D. Jia, X. Zhang, Y. Hou, R. Li and J. Wang, *International Journal of Machine Tools and Manufacture*, 122 (2017) 55.
3. S.G. Musharraf, W. Mazhar and N. Kanwal, *Chemistry Central Journal*, 7 (2013) 1.
4. Z. Huang, P. Luo, H. Zheng and Z. Lyu, *Ceramics International*, 48 (2022) 18765.
5. P. Kintz, L. Gheddar and J.S. Raul, *Drug Testing and Analysis*, 13 (2021) 1445.
6. M. Alimanesh, J. Rouhi and Z. Hassan, *Ceramics International*, 42 (2016) 5136.
7. H. Karimi-Maleh, R. Darabi, M. Shabani-Nooshabadi, M. Baghayeri, F. Karimi, J. Rouhi, M. Alizadeh, O. Karaman, Y. Vasseghian and C. Karaman, *Food and Chemical Toxicology*, 162 (2022) 112907.
8. J. Rouhi, C.R. Ooi, S. Mahmud and M.R. Mahmood, *Electronic Materials Letters*, 11 (2015) 957.
9. F.N. Karimooy, A.E. Bideskan, A.M. Pour and S.M. Hoseini, *Biomolecular Concepts*, 10 (2019) 73.
10. Y. Wang, C. Li, Y. Zhang, M. Yang, B. Li, L. Dong and J. Wang, *International Journal of*

- Precision Engineering and Manufacturing-Green Technology*, 5 (2018) 327.
11. P.M. Stepień, K. Reczko, A. Wieczorek, D. Zarębska-Michaluk, P. Pabjan, T. Król and W. Kryczka, *Clinical and experimental hepatology*, 1 (2015) 30.
  12. M.-R. Wang, L. Deng, G.-C. Liu, L. Wen, J.-G. Wang, K.-B. Huang, H.-T. Tang and Y.-M. Pan, *Organic letters*, 21 (2019) 4929.
  13. F. Husairi, J. Rouhi, K. Eswar, A. Zainurul, M. Rusop and S. Abdullah, *Applied Physics A*, 116 (2014) 2119.
  14. A. Büttner and D. Thieme, *Doping in Sports: Biochemical Principles, Effects and Analysis*, (2010) 459.
  15. M. Yang, C. Li, Y. Zhang, D. Jia, R. Li, Y. Hou, H. Cao and J. Wang, *Ceramics International*, 45 (2019) 14908.
  16. K.M. Shimko, J.W. O'Brien, L. Barron, H. Kayalar, J.F. Mueller, B.J. Tschärke, P.M. Choi, H. Jiang, G. Eaglesham and K.V. Thomas, *Drug testing and analysis*, 11 (2019) 937.
  17. J. Zhang, C. Li, Y. Zhang, M. Yang, D. Jia, G. Liu, Y. Hou, R. Li, N. Zhang and Q. Wu, *Journal of Cleaner Production*, 193 (2018) 236.
  18. I.M. Reddy, A. Beotra, S. Jain and S. Ahi, *Indian J Pharmacol*, 41 (2009) 80.
  19. W.M. Mück and J.D. Henion, *Biomed Environ Mass Spectrom*, 19 (1990) 37.
  20. A. Leinonen, T. Kuuranne, T. Kotiaho and R. Kostianen, *Steroids*, 69 (2004) 101.
  21. L. Göschl, G. Gmeiner, P. Gärtner, G. Stadler, V. Enev, M. Thevis, W. Schänzer, S. Guddat and G. Forsdahl, *Drug Testing and Analysis*, 13 (2021) 1668.
  22. G. Conneely, D. O'Mahony, H. Lu, G. Guilbault, M. Pravda and M. Aherne, *Analytical letters*, 40 (2007) 1280.
  23. G. Becskereki, G. Horvai and B. Tóth, *Polymers (Basel)*, 13 (2021) 1781.
  24. Z. Zhang, Y. Li, X. Liu, Y. Zhang and D. Wang, *International journal of electrochemical science*, 13 (2018) 2986.
  25. B. Liu, Y. Ma, F. Zhou, Q. Wang and G. Liu, *International Journal of Electrochemical Science*, 15 (2020) 9590.
  26. Q. Zeng, X. Huang and M. Ma, *International journal of electrochemical science*, 12 (2017) 3965.
  27. Y. Wang, L. Yao, X. Liu, J. Cheng, W. Liu, T. Liu, M. Sun, L. Zhao, F. Ding and Z. Lu, *Biosensors and Bioelectronics*, 142 (2019) 111483.
  28. R. Paul, P. Kumbhakar and A.K. Mitra, *Journal of Experimental Nanoscience*, 5 (2010) 363.
  29. R. Rahimpoor, A. Firoozichahak, S. Alizadeh, D. Soleymani-Ghoozhdhi and F. Mehregan, *RSC Advances*, 12 (2022) 16267.
  30. J. Rouhi, S. Mahmud, S.D. Hutagalung and S. Kakooei, *Journal of Micro/Nanolithography, MEMS, and MOEMS*, 10 (2011) 043002.
  31. X. Zhao, L. Chen and B. Li, *Food chemistry*, 255 (2018) 226.
  32. M. Liu, C. Li, Y. Zhang, Q. An, M. Yang, T. Gao, C. Mao, B. Liu, H. Cao and X. Xu, *Frontiers of Mechanical Engineering*, 16 (2021) 649.
  33. S. Zheng, W. Smit, A. Spannenberg, S. Tin and J.G. de Vries, *Chemical Communications*, 58 (2022) 4639.
  34. X. Wu, C. Li, Z. Zhou, X. Nie, Y. Chen, Y. Zhang, H. Cao, B. Liu, N. Zhang and Z. Said, *The International Journal of Advanced Manufacturing Technology*, 117 (2021) 2565.
  35. H. Dai, D. Xiao, H. He, H. Li, D. Yuan and C. Zhang, *Microchimica Acta*, 182 (2015) 893.
  36. L. Nan, C. Yalan, L. Jixiang, O. Dujuan, D. Wenhui, J. Rouhi and M. Mustapha, *RSC Advances*, 10 (2020) 27923.
  37. Y. Wu, P. Deng, Y. Tian, Z. Ding, G. Li, J. Liu, Z. Zuberi and Q. He, *Bioelectrochemistry*, 131 (2020) 107393.
  38. R. Savari, J. Rouhi, O. Fakhar, S. Kakooei, D. Pourzadeh, O. Jahanbakhsh and S. Shojaei, *Ceramics International*, 47 (2021) 31927.

39. Z. Savari, S. Soltanian, A. Noorbakhsh, A. Salimi, M. Najafi and P. Servati, *Sensors and Actuators B: Chemical*, 176 (2013) 335.
40. M. Yang, C. Li, Z. Said, Y. Zhang, R. Li, S. Debnath, H.M. Ali, T. Gao and Y. Long, *Journal of Manufacturing Processes*, 71 (2021) 501.
41. G. Cirillo, S. Hampel, F. Puoci, D. Haase, M. Ritschel, A. Leonhardt, F. Iemma and N. Picci, *Materials science and technology*, (2012) 181.
42. H. Karimi-Maleh, H. Beitollahi, P.S. Kumar, S. Tajik, P.M. Jahani, F. Karimi, C. Karaman, Y. Vasseghian, M. Baghayeri and J. Rouhi, *Food and Chemical Toxicology*, (2022) 112961.
43. C. Liu and J. Rouhi, *RSC Advances*, 11 (2021) 9933.
44. N.I.K. Deshmukh, G. Zachar, A. Petróczi, A.D. Székely, J. Barker and D.P. Naughton, *Chemistry Central Journal*, 6 (2012) 162.
45. J.M. Sila, P.M. Guto, I.N. Michira and F.B. Mwaura, *International Journal of Sciences: Basic and Applied Research (IJSBAR)*, 40 (2018) 220.
46. T. Gao, C. Li, Y. Wang, X. Liu, Q. An, H.N. Li, Y. Zhang, H. Cao, B. Liu and D. Wang, *Composite Structures*, 286 (2022) 115232.
47. B. Li, C. Li, Y. Zhang, Y. Wang, D. Jia and M. Yang, *Chinese Journal of Aeronautics*, 29 (2016) 1084.
48. Z. Zhao, C. Huang, Z. Huang, F. Lin, Q. He, D. Tao, N. Jaffrezic-Renault and Z. Guo, *TrAC Trends in Analytical Chemistry*, 139 (2021) 116253.

© 2022 The Authors. Published by ESG ([www.electrochemsci.org](http://www.electrochemsci.org)). This article is an open access article distributed under the terms and conditions of the Creative Commons Attribution license (<http://creativecommons.org/licenses/by/4.0/>).